

# *Supporting Information*

## **Charge Generation and Recombination in Fullerene-Attached Poly(3-hexylthiophene)-Based Diblock Copolymer Films**

*Shunsuke Yamamoto<sup>a,†</sup>, Hiroaki Yasuda<sup>a</sup>, Hideo Ohkita<sup>a,b,\*</sup>, Hiroaki Bente<sup>a</sup>, Shinzaburo Ito<sup>a</sup>, Shoji  
Miyanishi<sup>c,‡</sup>, Keisuke Tajima<sup>c,d</sup>, and Kazuhito Hashimoto<sup>c</sup>*

<sup>a</sup> Department of Polymer Chemistry, Graduate School of Engineering, Kyoto University, Katsura,  
Nishikyo-ku, Kyoto 615-8510, Japan.

<sup>b</sup> Japan Science and Technology Agency (JST), PRESTO, 4-1-8 Honcho Kawaguchi, Saitama 332-  
0012, Japan.

<sup>c</sup> Department of Applied Chemistry, School of Engineering, The University of Tokyo, 7-3-1 Hongo,  
Bunkyo-ku, Tokyo 113-8656, Japan.

<sup>d</sup> RIKEN Center for Emergent Matter Science, 2-1 Hirosawa, Wako, Saitama 351-0198 Japan.

\*E-mail: ohkita@photo.polym.kyoto-u.ac.jp. Tel.: +81 75 383 2613. Fax: +81 75 383 2617

## Complete Author List for Ref 2 and 12

(2) You, J.; Dou, L.; Yoshimura, K.; Kato, T.; Ohya, K.; Moriarty, T.; Emery, K.; Chen, C.-C.; Gao, J.; Li, G.; Yang, Y. A Polymer Tandem Solar Cell with 10.6% Power Conversion Efficiency. *Nat. Commun.* **2013**, *4*, 1446.

(12) Johnson, K.; Huang, Y.-S.; Huettner, S.; Sommer, M.; Brinkmann, M.; Mulherin, R.; Niedzialek, D.; Beljonne, D.; Clark, J.; Huck, W. T. S.; Friend, R. H. Control of Intrachain Charge Transfer in Model Systems for Block Copolymer Photovoltaic Materials. *J. Am. Chem. Soc.* **2013**, *135*, 5074–5083.

## Transient Absorption Measurements

The femtosecond transient absorption data were collected with a pump and probe transient absorption spectroscopy system (Ultrafast Systems, Helios). The pump light was second harmonic pulses (400 nm, fwhm 100 fs, 500 Hz) from a regeneratively amplified Ti-sapphire laser (Spectra-Physics, Hurricane). The probe beam was detected with a linear CCD array (Ultrafast Systems, SPEC-VIS) for the visible wavelength range from 400 to 900 nm and with a digital line scan InGaAs camera (Ultrafast Systems, SPEC-NIR) for the near-IR wavelength range from 850 to 1600 nm. The typical noise level of this system is lower than  $2 \times 10^{-4}$ .

For the microsecond transient absorption measurement, the sample was excited with a light pulse (500 nm, 4 Hz) from a dye laser (Photon Technology International, GL-301) that was pumped with a nitrogen laser (Photon Technology International, GL-3300), and probed with a monochromatic light from a 50-W quartz tungsten halogen lamp (Thermo-ORIEL, Model 66997) with a light intensity controller (Thermo-ORIEL, Model 66950), which was equipped with appropriate optical cut-filters and two monochromators (Ritsu, MC-10N) before and after the sample to reduce stray light, scattered light, and emission from the sample. The probe light was detected with a pre-amplified Si photodiode (Costronics Electronics). The detected signal was sent to the main amplification system with an electronic band-pass filter (Costronics Electronics) to improve the noise-to-signal ratio. The amplified signal was collected with a digital oscilloscope (Tektronix, TDS2022), which was synchronized with a trigger signal of the laser pulse from a photodiode (Thorlabs, DET10A). The detectable absorbance change  $\Delta OD$  is as small as  $\sim 10^{-5} - 10^{-6}$  depending on the measuring time domain. For the white bias light source, a 150W-Xe lamp (Kenko Tokina, XEF-152S) was used.

## Device Parameters

**Table S1.** Photovoltaic parameters of P3HT-PCBM copolymer solar cells.<sup>[S1]</sup>

	$J_{SC} / \text{mA cm}^{-2}$	$V_{OC} / \text{V}$	FF	PCE / %
P3HT/PCBM	8.61	0.54	0.66	3.07
P3HT-PCBM	8.14	0.48	0.63	2.46

In this study, we employed the same P3HT-PCBM diblock polymer. The fabrication condition of films was also the same as that reported previously.<sup>[S1]</sup>

## Transient Absorption Spectrum of Singlet Excitons in P3HT

**Figure S1a** shows the transient absorption spectra of a P3HT neat film measured under an excitation fluence similar to that in Figure 3. On the basis of the initial spectrum at 0 ps, the ratio of extinction coefficients of the singlet exciton at 1000 and 1200 nm  $\varepsilon_{1000}/\varepsilon_{1200}$  is estimated to be 0.506. In the main text, the polaron formation dynamics is extracted assuming that the ratio is independent of time. As shown in the figure, however, the singlet exciton band is shifted with time. In other words, the ratio is also dependent on time. More correctly, the polaron formation dynamics should be extracted by using time-dependent ratio of extinction coefficients. Figure S1b shows the temporal evolution of the ratio of  $\Delta OD$  at 1000 and 1200 nm. Considering the time-dependent ratio, the polaron generation dynamics can be extracted by the following equation:

$$\Delta OD_{\text{polaron}}^c(t) = \Delta OD_{1000} - \Delta OD_{1200} \times \Delta OD_{1000,\text{neat}}(t)/\Delta OD_{1200,\text{neat}}(t) \quad (\text{S1})$$

As shown in the **Figure S2**, the corrected polaron formation dynamics  $\Delta OD_{\text{polaron}}^c(t)$  is identical to  $\Delta OD_{\text{polaron}}$  shown in Figure 4. We conclude that the spectral shift has negligible impact on the analysis of the polaron generation dynamics described in the main text.

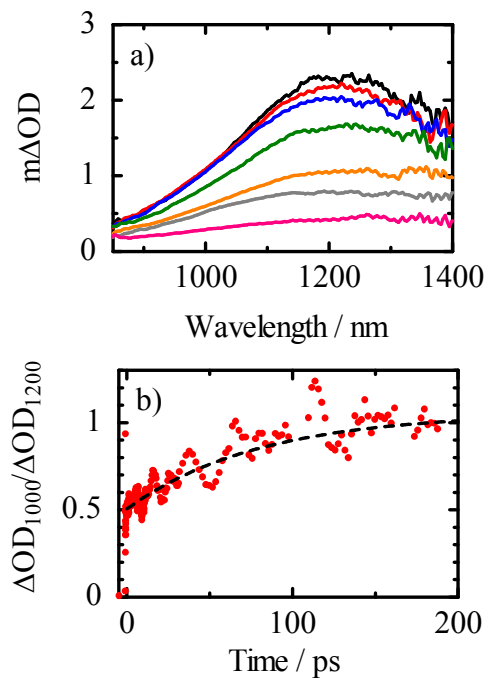


**Figure S1.** a) Transient absorption spectrum of P3HT neat films 0 (black), 1 (red), 2 (blue), 10 (green), 50 (orange), 100 (gray), and 200 ps (pink) after the excitation and b) the ratio of transient absorption decay monitored at 1000 and 1200 nm after the later excitation at 400 nm. The broken line shows the exponential fitting for the data:  $\Delta OD_{1000,neat}(t)/\Delta OD_{1200,neat}(t) = 0.506 + 0.550 [1 - \exp(-t/80)]$ .

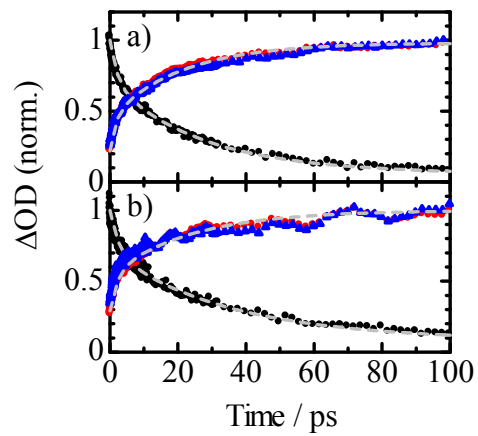


**Figure S2.** Polaron generation dynamics: The black and red circles shows  $\Delta OD$  without correction plotted in Figure 4 and the blue triangles shows  $\Delta OD_{\text{polaron}}^c$  with correction as described in the Supporting Information.

## Detailed Kinetic Parameters for Transient Decay Analyses

**Table S2.** Fitting parameters for the transient absorption decay of singlet exciton signals. (Figure 4)

	$A_1 / \%$	$\tau_1 / \text{ps}$	$A_2 / \%$	$\tau_2 / \text{ps}$	$A_3 / \%$
P3HT/PCBM	62	26	29	2.1	9
P3HT-PCBM	58	32	29	2.4	13

**Table S3.** Fitting parameters for the transient absorption decay of polaron signals. (Figure 4)

	$B_1 / \%$	$\tau_3 / \text{ps}$	$B_2 / \%$	$\tau_4 / \text{ps}$	$B_3 / \%$
P3HT/PCBM	54	21	24	1.6	22
P3HT-PCBM	45	26	26	2.0	28

**Table S4.** Fitting parameters for the time evolution of the bleaching signals (Figure 5) in P3HT/PCBM blend and P3HT-PCBM copolymer films.

	$C_1 / \%$	$\tau_{\text{cry}} / \text{ps}$	$C_2 / \%$	$D_1 / \%$	$\tau_{\text{a1}} / \text{ps}$	$D_2 / \%$	$\tau_{\text{a2}} / \text{ps}$	$D_3 / \%$
P3HT/PCBM	40	300	60	41	300	0	–	59
P3HT-PCBM	29	310	71	22	300	36	31	42

## Transient Absorption Spectra upon Excitation at 500 nm

**Figure S3** shows the transient absorption spectra of P3HT/PCBM blend and P3HT-PCBM copolymer films excited at 500 nm. Note that the block copolymer for this measurement is slightly different in the monomer sequence from that employed in the main text but identical to that reported in Ref S2. As shown in the figure, both the singlet exciton and the photobleaching bands decreased to less than half of the initial signal, suggesting that the decay is due to singlet–singlet exciton annihilation. In other words, more than half of singlet excitons just deactivate to the ground state because of the singlet–singlet exaction annihilation even at the lowest excitation fluence for the clear observation of charge carriers. This is probably because P3HT fraction is as large as 62.5% in the films. Thus, we focus on the transient absorption upon the excitation not at 500 nm but at 400 nm to discuss the charge generation dynamics in details. Interestingly, we note that there is no distinct difference in the P3HT polaron band at 3 ns between P3HT/PCBM blend and P3HT-PCBM copolymer films. This finding suggests that there is no additional charge generation loss in P3HT-PCBM copolymer films upon the excitation of P3HT crystalline domains at 500 nm, which is different from that upon the excitation of P3HT amorphous domains at 400 nm.

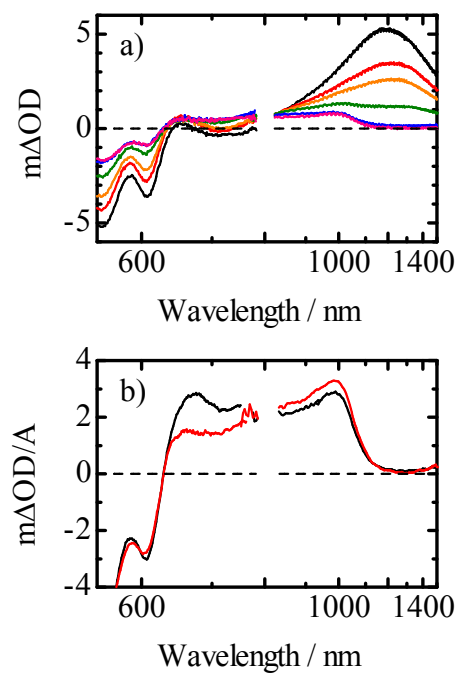


**Figure S3.** a) Transient absorption spectra of P3HT-PCBM block copolymer films 0 (black), 1 (red), 2 (orange), 10 (green), and 100 ps (blue) after the later excitation at 500 nm. The fluence was set to  $5 \mu\text{J cm}^{-2}$ . The broken lines show the baseline. b) Transient absorption spectra of P3HT/PCBM blend (black) and P3HT-PCBM copolymer films (red) 3 ns after the excitation at 500 nm. The transient signals were corrected for variation in the absorption at the excitation wavelength.

## Bimolecular Recombination Dynamics

For the discussion of charge carrier lifetime in relation to the device performance, the charge carrier lifetime should be evaluated under the same charge carrier density under the device operation conditions. We therefore evaluate the charge carrier lifetime from the transient absorption decay under continuous white light bias ( $100 \text{ mW cm}^{-2}$ ) in the main text. Under the white light bias at  $100 \text{ mW cm}^{-2}$ , the steady-state density of charge carriers  $n_{\text{bias}}$  is as high as of the order of  $10^{16} \text{ cm}^{-3}$ ,<sup>[S3]</sup> which is much larger than the transient density of charge carriers induced by weak laser pulses  $\Delta n(t)$ . Thus, the decay dynamics of the laser-induced carrier density  $\Delta n(t)$  is followed by a pseudo-first-order kinetics; and consequently, the pseudo-first-order lifetime can be considered as the charge carrier lifetime at  $n \approx 10^{16} \text{ cm}^{-3}$  under the device operation condition. We used this lifetime  $\tau_C$  in the discussion for the charge collection in the main text for the sake of simplicity.

For more precise evaluation of the lifetime of total charge carriers, the reaction order or the recombination reaction should be taken into account: the charge carrier lifetime of total charge carriers  $\tau_n$  is given by  $\tau_n = (1 + \lambda)\tau_C$  where  $\lambda$  is estimated from the inverse of the exponent  $\alpha$  of the decay dynamics without the white light bias.<sup>[S4]</sup> In order to estimate the exponent  $\alpha$ , we also measured transient absorption without the white light bias. **Figure S4** shows the transient absorption spectra without continuous white light bias. These bands are safely assigned to P3HT polarons in ordered (700 nm) and disordered (1000 nm) domains as reported previously.<sup>[S1]</sup> **Figure S5** shows the decay dynamics of these polarons under various excitation intensities. All these decays are well explained by the empirical power-law function  $\Delta OD(t) = \Delta OD_0(1 + at)^{-\alpha}$  where  $\Delta OD_0$  is the initial signal amplitude, and  $a$  and  $\alpha$  are parameters. From the fitting, the exponent  $\alpha$  is obtained as indicated in the figure, reflecting the difference in the bimolecular recombination dynamics.<sup>[S5]</sup> From these parameters, the lifetime of total charge carriers  $\tau_n$  is estimated to be  $\tau_n = 65 \text{ }\mu\text{s}$  (P3HT-PCBM copolymer film), which is longer than  $\tau_n = 27 \text{ }\mu\text{s}$  (P3HT/PCBM blend film). In other words, the discussion in the text remains the same.

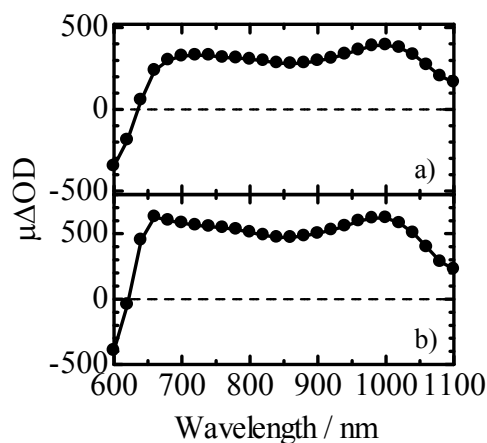


**Figure S4.** Transient absorption spectra of a) P3HT/PCBM blend and b) P3HT-PCBM copolymer films at 0.5  $\mu\text{s}$  after the laser excitation at 500 nm with a fluence of  $0.3 \mu\text{J cm}^{-2}$  without the white light bias.

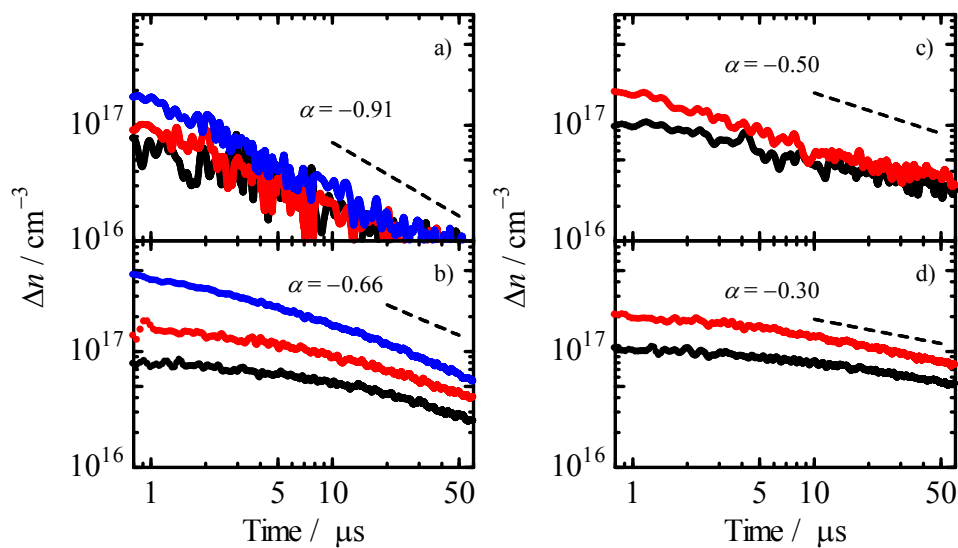


**Figure S5.** Transient absorption decays in P3HT/PCBM blend (a,c) and P3HT-PCBM copolymer (b,d) films probed at 700 (a,b) and 1000 (c,d) nm after the laser excitation at 500 nm with various fluencies of 5 (blue), 1 (red) and  $0.5 \mu\text{J cm}^{-2}$  (black) without the white light bias. The broken lines show the power law decay with an exponent of  $\alpha$  shown in the figure.

## REFERENCES

- (S1) Miyanishi, S.; Zhang, Y.; Hashimoto, K.; Tajima, K. Controlled Synthesis of Fullerene-Attached Poly(3-alkylthiophene)-Based Copolymers for Rational Morphological Design in Polymer Photovoltaic Devices. *Macromolecules* **2012**, *45*, 6424–6437.
- (S2) Miyanishi, S.; Zhang, Y.; Tajima, K.; Hashimoto, K. Fullerene Attached All-Semiconducting Diblock Copolymers for Stable Single-Component Polymer Solar Cells. *Chem. Commun.* **2010**, *46*, 6723–6725.
- (S3) Credgington, D.; Durrant, J. R. Insights from Transient Optoelectronic Analyses on the Open-Circuit Voltage of Organic Solar Cells. *J. Phys. Chem. Lett.* **2012**, *11*, 1465–1478.
- (S4) Shuttle, C.; Ballantyne, A.; Nelson, J.; Bradley, D.; Durrant, J. Bimolecular Recombination Losses in Polythiophene: Fullerene Solar Cells. *Phys. Rev. B* **2008**, *78*, 113201.
- (S5) Guo, J.; Ohkita, H.; Yokoya, S.; Benten, H.; Ito, S. Bimodal Polarons and Hole Transport in Poly(3-hexylthiophene):Fullerene Blend Films. *J. Am. Chem. Soc.* **2010**, *132*, 9631–9637.